Morphology of Calcite (CaCO3) Crystals Growing from Aqueous Solutions in the Presence of Li+ Ions. Surface Behavior of the {0001} Form

ARTICLE *in* CRYSTAL GROWTH & DESIGN · MARCH 2004

Impact Factor: 4.89 · DOI: 10.1021/cg034217r

6 AUTHORS, INCLUDING:

Linda Pastero
Università degli Studi di Torino
71 PUBLICATIONS **352** CITATIONS
SEE PROFILE

Marco Bruno
Università degli Studi di Torino
84 PUBLICATIONS **706** CITATIONS
SEE PROFILE

Marco Rubbo
Università degli Studi di Torino
98 PUBLICATIONS **614** CITATIONS
SEE PROFILE

Dino Aquilano
Università degli Studi di Torino
190 PUBLICATIONS **1,000** CITATIONS
SEE PROFILE

CRYSTAL GROWTH & DESIGN
2004
VOL. 4, NO. 3
485−490

Morphology of Calcite ($CaCO_3$) Crystals Growing from Aqueous Solutions in the Presence of Li^+ Ions. Surface Behavior of the {0001} Form

Linda Pastero, Emanuele Costa, Marco Bruno, Marco Rubbo, Giulio Sgualdino,‡ and Dino Aquilano*,†

Dipartimento di Scienze Mineralogiche e Petrologiche, Università degli Studi di Torino, via V. Caluso 35 - 10125 - Torino, Italy, and Dipartimento Chimico, Università degli Studi di Ferrara, via L. Borsari 46-44100, Ferrara, Italy

Received November 13, 2003; Revised Manuscript Received February 26, 2004

ABSTRACT: Calcite crystals were nucleated and grown from supersaturated aqueous solutions in the presence of variable concentrations of lithium. The diagram of supersaturation vs $[Li^+]/[Ca^{2+}]$ concentration ratio ("morphodrome") shows a continuous habit variation, from the dominant $\{01\bar{1}1\}$ rhombohedron (at low $[Li^+]/[Ca^{2+}]$ ratio) to the dominant {0001} form (at high $[Li^+]/[Ca^{2+}]$ ratio). The morphological change is interpreted in terms of two-dimensional layers having the structure of the monoclinic Li_2CO_3 crystal which are epitaxially adsorbed on the restructured {0001} form of calcite. Hence, even if {0001} is a K form (in the sense of Hartman-Perdok), the corresponding surface behaves like a F form, growing layer by layer from low to high supersaturation values.

1. Introduction

The effect of adding lithium to aqueous solutions supersaturated with respect to calcite, at room temperature and pressure, is known since the paper of Rajam and Mann[1] who found that the morphology of growing crystals is not only built by the $\{10\bar{1}4\}$cleavage rhombohedron but also by the {0001} pynacoid. Moreover, they observed that the importance of this form increases when the $[Ca^{2+}]/[Li^+]$ ratio decreases from 0.5 to 0.05. From IR spectroscopic analysis, it was also argued that Li^+ ions cannot be segregated within the bulk of the growing crystals but can be adsorbed on the {0001} surface sites so hindering their advancement.

More recently, Nefyodova et al.[2] starting from $\{10\bar{1}4\}$ seeds, obtained calcite crystals grown under hydrothermal conditions from NH_4Cl and NH_4Br solutions. Their growth morphology was enriched by the acute $\{01\bar{1}2\}$ rhombohedron and the $\{11\bar{2}0\}$ prismatic form. However, the addition of lithium to these solutions led to the development of the {0001} form.

Simulation of the effect of lithium on the equilibrium morphology of calcite was achieved by replacing surface Ca^{2+} ions with Li^+ and calculating the influence on the surface energy.[3−5] The calculated segregation energy of lithium ions on the (0001) face was −776.1 kJ mol^{-1} with respect to the bulk and −407.9 kJ mol^{-1} in solution, indicating the preference of lithium to remain at the crystal surface.

Hence, there are both experimental evidence and theoretical grounds to assert that lithium plays an important role as a habit modifier of calcite, even though the literature data are rather qualitative and the impurity effect is not distinguished from that of supersaturation.

This work becomes a part of a research program we started some time ago on equilibrium and growth morphology of calcium carbonates.[6−12] In this paper, we aim at obtaining quantitative information about the lithium effect on the morphology of calcite growing under well-defined supersaturation values at room temperature and pressure, when the amount of Li^+ in solution varies within a well-defined range of concentration. Further, we will attempt to interpret the morphological modifications due to the stabilization of the {0001}form in terms of epitaxy, which should set up between a 2D layer of lithium carbonate (Li_2CO_3) and the restructured (0001) face of calcite.

2. Experimental Procedures

Growth experiments have been carried out using deionized water free of CO_2, by mixing calcium, lithium, and carbonate concentrated mother solutions. Analytical grade reagents were employed. Concentrations of mother solutions ranged between 2 and 800 mM in $CaCl_2 \cdot H_2O$, from 0.1 to 16 mM in $NaHCO_3$, and from 0 to 3.25 M in LiCl. Solutions were always stirred after mixing. A set of experiments has been performed varying both Li^+ concentration and supersaturation; then three series of growth runs have been carried out, at constant supersaturation values, varying the $[Li^+]/[Ca^{2+}]$ ratio to check the effect of Li^+ concentration on crystal morphology. Crystals were collected on glass slices and then studied by optical microscopy, scanning electron microscopy (Cambridge Stereoscan 3600), and atomic force microscopy (Digital Instruments Nanoscope III equipped with a 12 μm scanner and DME Dualscope C21 equipped with a 50 μm scanner).

2.1. Chemical Equilibria and Supersaturations in Lithium Bearing Solutions. Calcite supersaturation was defined as

$$\beta = \frac{a_{Ca^{2+}} a_{CO_3^{2-}}}{K_{sp}}$$

where a indicates the species activity and K_{sp} is the solubility product of calcite ($K_{sp} = 3.84 \times 10^{-9}$). Species abundance in aqueous solution was calculated at 20 °C and 1 bar. The species considered in the model system were H^+, OH^-, Li^+, Na^+, Ca^{2+}, Cl^-, HCO_3^-, CO_3^{2-}, $CaHCO_3$, $CaOH^+$, $CaCl^+$, CO_2^0, $CaCl_2^0$, $LiCl^0$, $LiOH^0$, $NaOH^0$, HCl^0, $CaCO_3^0$, $CaCO_3$ (calcite), and H_2O (liquid); the apex 0 represents aqueous associations.

* Corresponding author. E-mail address: dino.aquilano@unito.it.
† Università degli Studi di Torino.
‡ Università degli Studi di Ferrara.

10.1021/cg034217r CCC: $27.50
Published on Web 03/30/2004

Scheme 1. Linearly Independent Reactions Describing the Equilibria in the System

1) $2CaHCO_3^+ + CO_3^{2-} \leftrightarrow H_2O(l) + CO_2^0 + 2CaCO_3^0$

2) $2HCO_3^- \leftrightarrow H_2O(l) + CO_2^0 + CO_3^{2-}$

3) $Ca_2^+ + CO_3^{2-} \leftrightarrow CaCO_3^0$

4) $2CaOH^+ + CO_2^0 + CO_3^{2-} \leftrightarrow H_2O(l) + 2\,CaCO_3^0$

5) $2OH^- + CO_2^0 \leftrightarrow H_2O(l) + CO_3^{2-}$

6) $2H^+ + CO_3^{2-} \leftrightarrow H_2O(l) + CO_2^0$

7) $CaCO_3^0 \leftrightarrow CaCO_3(\text{calcite})$

8) $CaCl_2^0 + CO_3^{2-} \leftrightarrow CaCO_3^0 + 2Cl^-$

9) $LiCl^0 \leftrightarrow Li^+ + Cl^-$

10) $2LiOH^0 + CO_2^0 \leftrightarrow H_2O(l) + CO_3^{2-} + 2Li^+$

11) $2NaOH^0 + CO_2^0 \leftrightarrow H_2O(l) + CO_3^{2-} + 2Na^+$

12) $2HCl^0 + CO_3^{2-} \leftrightarrow H_2O(l) + CO_2^0 + 2Cl^-$

13) $CaCl^+ + CO_3^{2-} \leftrightarrow CaCO_3^0 + Cl^-$

Linearly independent reactions, which entirely describe the equilibria in the system, are quoted in Scheme 1.

The calcite supersaturation and the species abundance were determined by minimizing the Gibbs function (G) of the system, at constant temperature, pressure, and abundance of elements:[13]

$$G = \sum_i \mu_i n_i \qquad (1)$$

where μ_i is the chemical potential of the ith species, calculated at the pressure and temperature of interest (1 bar and 20 °C) and n_i its mole number. The minimization is performed numerically by a sequential quadratic programming algorithm,[14] implemented in the NAG library FORTRAN.

The thermodynamic properties of the species were taken from the SLOP98 database.[15] The activity coefficients (γ_i) were calculated by means of the equation:[16a]

$$\ln \gamma_i = \frac{-Az_i^2\sqrt{I}}{1 + B\text{å}\sqrt{I}} + bI \qquad (2)$$

where I is the ionic strength, z_i is the ionic charge, å and b are constant for each ion (see Table 1); A and B are temperature depending solvent parameters (at 20 °C $A = 0.5064$, $B = 0.328$).[16b] Water was considered ideal.

Experiments were carried out in closed vessels and the initial β value ranged between 4 and 87. From the calculation of chemical equilibria, it is found that β values are only slightly affected by the Li^+ concentration: in fact, pure aqueous solutions have β values higher by only 2% with respect to that of the solution in which the concentration ratio $[Li^+]/[Ca^{2+}]$ reaches the value of 4.

2.2 Observed Growth Morphology of Bulky and Hollow Crystals. When variable amounts of Li^+ ions are added to the pure aqueous solutions, previously supersaturated with respect to calcite, the pynacoid {0001} and the vicinal {01$\bar{1}$1} rhombohedron enter enriching the growth morphology of bulky crystals which were built up by the sole {10$\bar{1}$4} cleavage rhombohedron when growing from pure solutions (under the same supersaturation values and $[Ca^{2+}]/[CO_3^{2-}]$ ratio) (see Figure 1a). Also crystal bubbles we obtained by nucleation and growth of calcite around gaseous cavities (previously nucleated in lithium bearing solutions[10−12]) showed the {0001} form, besides the dominant cleavage rhombohedron (see Figure 1b).

Table 1. Individual Ion Activity Coefficient Parameters in Equation 2[a]

ionic species	å	b
H^+	9.0	0
OH^-	3.5	0
Li^+	6.0	0
Na^+	4.0	0.075
Ca^{2+}	5.0	0.165
Cl^-	3.5	0.015
HCO_3^-	5.4	0
CO_3^{2-}	5.4	0
$CaHCO_3^+$	0	0
$CaOH^+$	0	0
$CaCl^+$	0	0

[a] Taken from ref 16b.

The morphological importance of the {0001} form increases when bulky crystals nucleate and grow, in a steady state, in the presence of increasing amounts of lithium. In such conditions, the crystal habit becomes more and more {0001} platy starting from an initial $[Li^+]/[Ca^{2+}]$ ionic concentration ratio equal to 0.01. This behavior is illustrated in Figure 2 where the steady-state morphologies are illustrated within the frame of a "morphodrome" (a diagram representing solution supersaturation versus $[Li^+]/[Ca^{2+}]$ ionic concentration ratio).

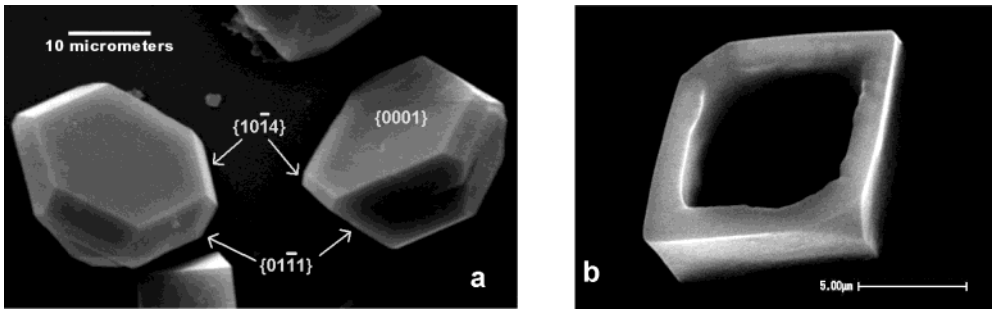

Figure 1. (a) Calcite crystals growing from aqueous solution in the presence of lithium ions. The growth morphology is characterized by the cleavage {1014} rhombohedron, the {0001} pynacoid, and the vicinal {01$\bar{1}$1} form; (b) calcite bubbles nucleated and grown in lithium bearing solutions show a small-sized {0001} form as well.

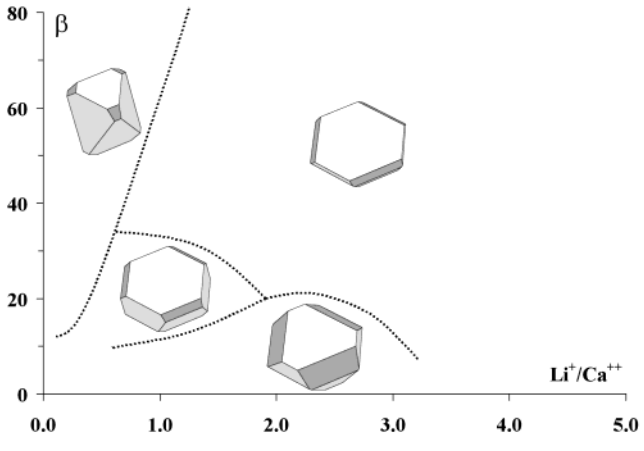

Figure 2. Steady-state growth morphology of calcite crystals grown under varying $[Li^+]/[Ca^{2+}]$ concentration ratio and supersaturation (morphodrome). Different domains are associated with the most frequent habit observed at a given initial supersaturation value and $[Li^+]/[Ca^{2+}]$ ratio.

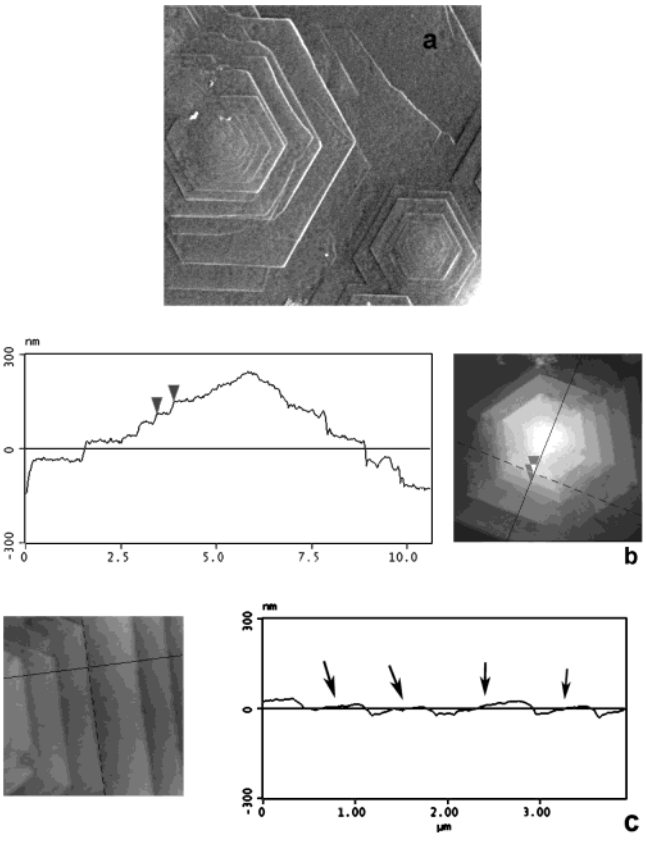

Figure 3. Surface structure of the {0001} calcite form. (a) Scanning electron micrograph showing pseudohexagonal growth hillocks. Macrosteps run along the <100> directions. (b) AFM images of an hillock along with its profile: the macrosteps thickness (small arrows) varies between 5 and 35 nm and the hillocks slope increases from 1° to 6.5° with increasing supersaturation. (AFM abscissa: μm). (c) Detailed AFM images of the profile of the terraces lying between successive macrosteps showing small cobbles (arrows) and the wavy surface structure.

In this paper, we will confine our attention to the {0001} form, owing to its high occurrence frequency in natural crystal and to the transition of character (from kinked to flat) that it undergoes when it grows in the presence of specific impurities such as Li^+ ions.[1] On the other hand, the $\{01\bar{1}1\}$ form is a vicinal one that looks more rounded than flat in synthetic crystals and very rarely occurs in natural environments.

2.3. Observed Surface Features of the {0001} Form. From scanning electron microscopy and atomic force microscopy observations, it is found that the {0001} form has layered surfaces within a wide range of supersaturations. A general ex-situ overview of crystals obtained at moderate β values ($4 < \beta < 37$) shows that the {0001} surfaces are populated by pseudohexagonal growth hillocks built by more or less periodic sequence of macrosteps (Figure 3a,b).

The mean step thickness varies between 5 and 35 nm and the hillocks slope increases from 1° to 6.5° with increasing supersaturation. Hence it can be said that under these conditions the kinetic behavior of {0001} form is that of an F-form.

It is worth remembering here that F $\{hkl\}$ forms are those which grow according to a layer mechanism and therefore, being slowly growing, become the most important ones in the growth morphology. Their profile is flat (F) and their kinetic behavior is due to the peculiar property that, within their d_{hkl} slices, at least two types of periodic bond chains (PCBs) between growth units can be found. On the contrary, when only one type of PBC runs within a given d_{hkl} slice, the corresponding face profile is stepped (S face) because there is no correlation during growth among all parallel bond chains. Hence S faces grow through one-dimensional nucleation. Finally, if a face does not contain any PBC in its d_{hkl} slice, its profile is kinked (K-face). It needs no nucleation at all: thus it grows fast and cannot normally be found in the crystal morphology (see, for a deeper understanding, ref 33).

Owing to the pollution affecting the sample surface during the ex-situ measurements, we cannot properly examine the hillocks top and prove, at the time being, that these hillocks are generated by spiral growth; nonetheless, the macrosteps periodicity speaks in favor of this hypothesis. Moreover, from a deeper analysis of the profile of the terraces lying between two successive macrosteps, it turns out that the terrace surfaces are not atomically flat. On the contrary, they are slowly wavy and populated by small cobbles whose height does not exceed a few nanometers, as illustrated in Figure 3b and, more clearly, in Figure 3c.

3. Restructuring the (0001) Surface. A Comparison with the {111} Octahedron of the NaCl Type Lattice

The analogies between the structures of rhombohedral carbonates (space group $R\bar{3}c$) and those of alkali halides with NaCl-type lattice (space group $Fm3m$) are striking, apart from angular distortion from cube to rhombohedron. In fact, if the planar CO_3^{2-} ion is considered as a point charge, the surface structure of the cleavage $\{10\bar{1}4\}$ calcite rhombohedron corresponds to that of the {100} NaCl cube, both structures consisting of positive and negative ions arranged alternately along rows parallel to the edges of the respective cells.

This reflects in the correspondence between the periodic bond chains (PBCs) of these forms: the strongest PBC of calcite runs along the $<\bar{4}41>$ rhombohedron edges and shows the same structure as the strongest PBC of NaCl, which is parallel to the <100> edges of the cube. Further, and the matter concerns us closely, the form {0001} of calcite shows the same surface structure of the {111} octahedron of NaCl. Their crystal slices allowed by the extinction rules have a thickness d_{0006} (for calcite) and d_{111} (for NaCl), and cannot be stable in the vapor phase. In fact, according to Stranski[17,18] and Bertaut[19] the alternating layers of positive and negative charges generate an infinite electric field near the crystal surface (as that resulting from a 2D infinite array of iso-oriented dipole moments). To remove this instability, a given number of vacant sites

should be created within the outermost slice (restructuring the face), to fulfill the Hartman's conditions[20] and to make finite the electric field near the surface of ionic crystals. Nevertheless, the resulting character of the reconstructed and stable faces (both for {111} octahedron of NaCl and {0001} of calcite) is that of a K (kinked) face in the sense of Hartman-Perdok.[33]

On the other hand, it is known that all alkali halides with NaCl − lattice growing either from pure or doped aqueous solutions can show, besides the {100} form, also the {111} octahedron.[21−29]

Concerning the form {0001} of calcite, it should be remembered that its occurrence frequency is near 17% in natural samples grown from solution, as it ensues from a statistical study we carried out on the rich morphologies observed by Goldsmith[30] and Sunagawa[31] on more than 2500 crystals. This is a rather astonishing feature for a kinked face. Studying the growth morphology of $NaNO_3$ (which is isostructural with calcite) growing by solvent evaporation from pure aqueous solution, Kern found that the {0001} form dominates the cleavage rhombohedron at high evaporation rates (and hence at high supersaturations).[24] Moreover, it was experimentally proved[32] that in pure medium growth the usual rhombohedral habit of calcite varies from thick to fine-tabular due to the considerable development of the {0001} form when an excess of CO_3^{2-} ions is present in solution.

Hence, the problem was to find the reasons why a K face of an ionic crystal could change from the instability (in vapor phase) to the stability (in solution). The question was soundly faced by the Kern's School during the 60s[25−29] for the NaCl-type crystals growing both from pure aqueous solution and in the presence of specific impurities, by assuming that the crystal can be viewed as built by an integer number of octopoles $(NaCl)_4$ whose electric field is finite at the reconstructed {111} surface. The outermost slice of the {111} form was restructured in such a way that it maintained only the 25% and the 75% of the crystal sites in the outermost layer and in its subsequent layer, respectively.

The octopole model allowed the building of stable steps of different heights on the restructured surface. Moreover, a solvent (water) adsorption model on the step ledges was elaborated, in which water molecules, treated as electric dipole, interact with the electric field generated by the crystal at its own surface. Water molecules were considered to continue the crystal structure (a lattice model of the solvent), the average molecular distance in liquid water (0.275 nm) being not too different from the mean distance (0.281 nm) between first neighbors in the NaCl lattice. Calculations[25,28] showed that water adsorption stabilizes the {111} form which then can grow layer by layer, as a flat (F) face, and compete with the {100} form, as it was found from growth experiments in pure aqueous solutions in which the supersaturation was the only cause of habit modification.[24]

The impurity effect on the NaCl habit was distinguished from that due to the solvent adsorption; Cd^{2+} was proved to be the most efficient ion, even at low concentration, in promoting the appearance of the {111} form during growth.[24,25] To explain that it was assumed[29,34,35] that {111} NaCl surfaces are covered by an epitaxial layer whose composition and d_{0003} thickness are those of $CdCl_2$ hexagonal bulky crystal. The epitaxy model was completed by Simon and Boistelle[36] who thoroughly explained the Cd^{2+} effect and showed that a 2D adsorption compound can form on {100}, {110}, and {111} NaCl forms as soon as the saturation of the Cd^{2+} adsorption isotherm is reached.[37a,b] This compound is the mixed salt $CdCl_2{\cdot}2NaCl{\cdot}3H_2O$ (space group $R\bar{3}m$); the parametric fit of its (0001) face with the (111) NaCl is excellent (≅ 1%) and the structure of its d_{0003} slice perfectly continues the structure of the (111) NaCl face irrespective of what ion (Na^+ or Cl^-) is occupying the outermost layer.

Concerning the change of character (from K to F) of the {0001} form of calcite, it is worth remembering the work of the Computational Solid State Chemistry Group of Bath University.[5,38,39] In these papers, neither experimental nor theoretical results obtained by Kern's School on alkali halides are taken into account. Nevertheless, the dipolar effect intrinsic to the flat profile of the unreconstructed {0001} surface was removed and γ_{0001}, the specific surface energy of this restructured face, was calculated, at 0 K, by the energy minimization method. Its value was found to be 2580 erg cm^{-2}, without surface relaxation and to range between 830 and 1600 erg cm^{-2} after surface relaxation, depending on the interatomic potential used in calculation. The outermost d_{0006} slice maintains its K character, because no PBC in this slice was created after reconstruction. On addition of lithium, the remaining surface calcium is replaced and the surface is charge compensated by adding lithium to the unoccupied calcium sites. Thus, the surface site density is restored and the corresponding γ_{0001} value is lowered to 320 erg cm^{-2}.[5]

Aiming at explaining the lithium effect on the appearance of the {0001} form of calcite, we will adopt the interpretative path proposed by the Kern's school. And because the platy {0001} crystals begins to occur when the Li^+ concentration becomes comparable to that of Ca^{2+} ions, we will reasonably concentrate our attention on the epitaxy model of the adsorbed (001)-Li_2CO_3 layer.

4. The (001)-Li_2CO_3/(0001)-$CaCO_3$ Epitaxial Model

Li_2CO_3 crystallizes, at room temperature and pressure, in the monoclinic system (space group $C2/c$), its cell parameters being $a_o = 0.839$ nm, $b_o = 0.500$ nm, $c_o = 0.621$ nm; $\beta = 114.50°$.[40] From a comparison between calcite and Li_2CO_3 structures (both viewed along their y axes), it may be easily seen that their geometrical misfit is very low. In fact, from the drawing shown in Figure 4 it follows that the calcite lattice vector [210] is parallel to the [100] vector of Li_2CO_3 and that the relative misfit between their moduli $|2a_o^{calcite} \cos 30°| = 0.864$ nm and $|a_o^{Li_2CO_3}| = 0.839$ nm is +2.9%, whereas the relative misfit between $|b_o^{calcite}| = 0.4989$ nm and $|b_o^{Li_2CO_3}| = 0.500$ nm, is only −0.2%.

This means that geometrical conditions for epitaxy between the (0001) face of the calcite crystal and the (001) layers of lithium carbonate are largely fulfilled. Another surprising geometric concordance, even not necessary for the epitaxy to occur, is that found between

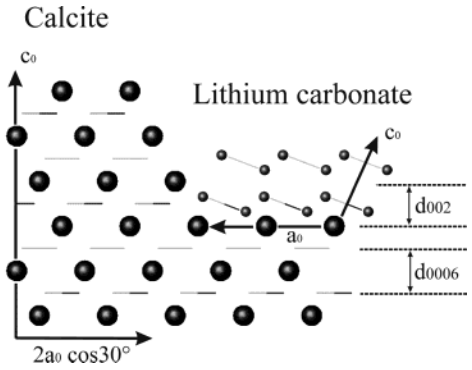

Figure 4. Projection of calcite (hexagonal frame) and Li_2CO_3 (monoclinic) along their [010] axis. Large and small spheres represent calcium and lithium atoms, respectively. Planar and alternate CO_3^{2-} groups are antiparallel; they do not lie parallel in the two structures, but the lattice coincidences in the common plane (0001 for calcite and 001 for Li_2CO_3) are extremely good (see text for details). Further, it is worth noting that the thickness of the elementary layers are the same in both structures, d_{0006} (for calcite) being practically equal to d_{002} (for Li_2CO_3).

the thickness of the d_{00l} layers of both structures. In fact, from systematic extinction rules it follows that the thickness allowed is $d_{0006} = 0.284$ nm and $d_{002} = 0.282$ nm for calcite and Li_2CO_3, respectively. Then the relative misfit does not reach 0.8%.

Concerning the structure of the epitaxial (001) layer of Li_2CO_3 it is worth noting that the outermost Li^+ ions, which should face the outermost (0001) layer of calcite, form a perfect 2D hexagonal lattice, as it follows from a projection of the Li_2CO_3 structure normal to the 001 plane. Outlining the details, Li^+ ions lie in the origin of the 2D space group $p6m$, the lattice vector corresponding to $b_o^{Li_2CO_3} = 0.5$ nm. This lattice coincides (misfit of 0.2%) with the lattice built by the vacant sites resulting from the second restructured layer of calcite (0001). In other words and remembering the reconstruction model of the {111} NaCl surfaces, we illustrated above, one can say that if the outermost calcite layer contains only the 25% of CO_3^{2-} ions, in the following one 75% of available sites will be occupied by Ca^{2+} ions while the Li^+ ions could fill the remaining ones.

Hence, an adsorbed Li_2CO_3 layer of thickness d_{002} can be structured on the (0001) face of calcite crystals. Within this layer, three PBCs develop: the strongest one is the [010] PBC, while the two others are the equivalent <110> PBCs.[41] The adsorbed layer behaves as a 2D crystal, which imposes its own PBCs to the underlying face.[42] In our particular case, the strong [010] PBC of the Li_2CO_3 adsorbed layer runs along the same direction of the [010] steps we observed and described above; moreover, owing to the 3-fold symmetry of the (0001) face of calcite, the adsorbed impurity shall impose three strong PBCs to the face which, in turn, transforms its character from kinked to flat (K → F transition).

5. Discussion

Kirov et al.[32] grew calcite crystals from pure aqueous solutions by the method of counterdiffusion of calcium and carbonate ions. An extension of the method was used, making possible the calcite crystallization in a medium containing calcium or carbonate ions in excess of their stoichiometric amounts in calcite. Crystals grown in the presence of an excess of Ca^{2+} ions exhibit an elongated habit determined by the prevailing development of some of the acute negative rhombohedra such as $\{01\bar{1}2\}$, $\{01\bar{1}1\}$ or $\{02\bar{2}1\}$, whereas with an excess of CO_3^{2-} ions the habit varies from thick to fine-tabular due to the considerable development of the {0001} form.

From Kirov's data one can also argue that the {0001} occurrence in pure aqueous solutions is not related to the supersaturation ratio (initial or not) but to the prevailing CO_3^{2-} concentration. To explain this effect and distinguish it from the habit modification due to the Li^+ adsorption, it is worth noting the role played by different growth mechanisms working on both $\{10\bar{1}4\}$ and {0001} forms, according to the scheme proposed first by Nielsen and Toft[43] and, successively, by van de Voort and Hartman.

Nielsen and Toft have shown that the growth rate of an electrolyte is a function of the ionic product as long as this growth rate is controlled by the rate of reaction (e.g., the deprotonation of the HCO_3^- group, or the kink dehydration...). This means that, for NaCl crystals, the growth rate of the (001) face increases when one of the ionic species is added to the solution. However, when the growth rate is controlled by diffusion, it is a function of the concentration of the electrolyte and not of the ionic product. So the growth rate does not change when the concentration of one of the species is increased. The growth rate has become a function of the concentration of the deficient species. This is the case for the restructured (111) face of NaCl. Hence, the growth rate of the cube increases, whereas that of the (111) face does not vary, which results in an increase of the morphological importance of the octahedron.[44]

The same reasoning could be applied to the competition between the cleavage rhombohedron and the {0001} form of calcite, when growing from pure solutions. It is well-known that the cleavage rhombohedron advance through spiral growth (mono- and two-layered) and that the rate determining process is either the ion integration in the kinks (a molecular jump and partial dehydration of a cation),[45−47] or the deprotonation of the HCO_3^- ion,[47] the parabolic law proving that $\{10\bar{1}4\}$ is a reaction-controlled form.

Concerning the growth mechanisms acting on the {0001} form of calcite crystals, we can propose the following interpretation path. In the pseudohexagonal layered patterns, we observed that, at low and intermediate supersaturation, the macrosteps run along the three equivalent <100> directions parallel to the intersections of the {0001} form with the cleavage rhombohedron. Their ledges should have the highly flat surface structure of the $\{10\bar{1}4\}$ form, while on the terraces there is a competition between two kinds of domains. One of them shows the features of a kinked face stabilized by water molecules adsorption while the other is built by two-dimensional islands of epitaxially and temporarily adsorbed Li_2CO_3, the small cobbles and the wavy structure observed on the terraces between successive macrosteps being the result of this competition. Then we must conjecture that the advancement rate of the step ledges on the terraces is partially hindered by the presence of these foreign islands, the

effect increasing as much as the $[Li^+]/[Ca^{2+}]$ concentration increases, for a given supersaturation value.

These considerations have to be verified by controlling that lithium has not been absorbed, as lithium carbonate, within the growth sector of the {0001} form, owing to the surprising coincidence between the thickness of the d_{0006} layer (for calcite) and d_{002} layer (for lithium carbonate) and, consequently, to the feasible overhanging of the calcite steps on the temporarily adsorbed lithium carbonate islands. To do that, measurements of adsorption isotherms of lithium on calcite have been planned along with the observation of the epitaxy of Li_2CO_3 bulky crystals on the {0001} form of calcite. We are also working at an accurate improvement of theoretical model employed in this paper.

Acknowledgment. We wish to thank Prof. Massimo Moret (University Milano-Bicocca) for the experience gained and the kind hospitality received in his AFM laboratory. We are also grateful to Prof. Hans Erik Lundager Madsen (University of Copenhagen) and to Prof. Francesco Abbona (this department) for useful discussions and help on determination of chemical equilibria.

References

(1) Rajam, S.; Mann, S. *J. Chem. Soc., Chem. Commun.* **1990**, 1789−1791.
(2) Nefyodova, I. V.; Lyutin, V. I.; Borodin, V. L.; Chvanski, P. P.; Leonyuk, N. I. *J. Cryst. Growth* **2000**, *211*, 458−460.
(3) Titiloye, J. O.; Parker, S. C.; Osguthorpe, D. G.; Mann, S. *J. Chem. Soc., Chem. Commun.* **1991**, 1494−1496.
(4) Kenway, P. R.; Oliver, P. M.; Parker, S. C.; Sayle, D. C.; Sayle, T. X. T.; Titiloye, J. O. *Mol. Simul.* **1992**, *9*, 83−98.
(5) Parker, S. C.; Kesley, E. T.; Oliver, P. M.; Titiloye, J. O. *Faraday Discuss.* **1993**, *95*, 75−84.
(6) Aquilano, D.; Rubbo, M. *Proceedings of the Italian Growth Conference. Transtech Publ. Ltd Mater. Sci. Forum* **1996**, *203*, 193−196.
(7) Aquilano, D.; Rubbo, M.; Catti, M.; Pavese, A. *J. Cryst. Growth* **1997**, *182*, 168−184.
(8) Rubbo, M.; Aquilano, D. *J. Cryst. Growth* **1998**, *194*, 156−159.
(9) Aquilano, D.; Calleri, M.; Natoli, E.; Rubbo, M.; Sgualdino, G. *Mater. Chem. Phys.* **2000**, *66*, 159−163.
(10) Aquilano, D.; Costa, E.; Genovese, A.; Massaro, F. R.; Pastero, L.; Rubbo, M. *J. Cryst. Growth* **2003**, *247*, 516−522.
(11) Pastero, L.; Costa, E.; Alessandria, B.; Rubbo, M.; Aquilano, D. *J. Cryst. Growth* 2003, *247*, 472−482.
(12) Aquilano, D.; Costa, E.; Genovese, A.; Massaro, F. R.; Rubbo, M. *Prog. Cryst. Growth Charact. Mater.* **2003**, *46*, 59−84.
(13) Smith, W. R.; Missen, R. W. *Chemical Reaction Equilibrium Analysis*; Wiley: New York, 1982.
(14) Gill, P. E.; Murray, W.; Wright, M. H. *User's Guide for SOL/NPSOL*; Report SOL 83-12, Stanford, California, 1983.
(15) Group Exploring Organic Processes In Geochemistry, Washington University (GEOPIG, http://epsc.wustl.edu/geopig).
(16) (a) Truesdell, A. H.; Jones, B. F. WATEQ, A Computer Program for Calculating Chemical Equilibria of Natural Waters; *U.S. Geol. Surv. J. Res.* **1974**, *2*, 233−348. (b) Nordstrom, D. K.; Munoz, J. L. *Geochemical Thermodynamics*, Benjamin/Cummings Publishing Co., Redwood City, CA, 1985; pp 198−204.
(17) Stranski, I. N. *Z. Phys. Chem.* **1928**, *A136*, 259−278.
(18) Stranski, I. N. *Z. Phys. Chem.* **1932**, *B17*, 127−135.
(19) Bertaut, F. *J. Phys. Radium* **1952**, *13*, 499−505.
(20) Hartman, P. *Bull. Soc. Franç. Minéral. Crist.* **1959**, *82*, 158−163.
(21) de Romé de l'Isle, J.-B. L. in *Cristallographie*; Paris, 1783; p 379.
(22) Johnsen, A. *Wachstum und Auflösung der Kristalle*; Engelmann, Leipzig, 1910.
(23) Spangenberg, G. *Z. Kristallogr.* **1924**, *59*, 383−405.
(24) (a) Kern, R. Thesis, University of Strasbourg, 1953. (b) Kern, R. *Bull. Soc. Franç. Minéral. Crist.* **1953**, *76*, 325−364. (c) Kern, R. *Bull. Soc. Franç. Minéral. Crist.* **1953**, *76*, 391−414.
(25) Boistelle, R. Thesis, University of Nancy, 1966.
(26) Bienfait, M.; Boistelle, R.; Kern, R. *C. R. Acad. Sci. Paris* **1963**, *256*, 2189−2193.
(27) Bienfait, M.; Boistelle, R.; Kern, R. *C. R. Acad. Sci. Paris*, **1964**, *258*, 880−883.
(28) Bienfait, M.; Boistelle, R.; Kern, R. in *Adsorption et Croissance Cristalline*, Colloq. Intern. CNRS, no. 152 , CNRS-Paris, 1965; pp 515−535.
(29) Bienfait, M.; Boistelle, R.; Kern, R. in *Adsorption et Croissance Cristalline*, Colloq. Intern. CNRS, no. 152, CNRS-Paris, 1965; pp 577−594.
(30) Goldschmidt, V. *Atlas der Kristallformen*; Universitatverlag, Heidelberg, 1923−1931; Vol. 1−9.
(31) Sunagawa, I. *Rep. Geol. Surv. Jpn* **1953**, *155*, 1−66.
(32) Kirov, G. K.; Vesselinov, I.; Cherneva, Z. *Kristall. Technik.* **1972**, *7*, 497−509.
(33) Hartman, P. in *Crystal Growth: An Introduction*; Hartman, P., Ed.; North-Holland, Amsterdam, 1973; pp 367−402.
(34) Royer, L. *C. R. Acad. Sci. Paris* **1934**, *198*, 185, 585, 949, 1869.
(35) Hartman, P. in *Adsorption et Croissance Cristalline*, Colloq. Intern. CNRS, no 152 CNRS-Paris, 1965; pp 477−513.
(36) Boistelle, R.; Simon, B. *J. Cryst. Growth* **1974**, *26*, 140−146.
(37) (a) Boistelle, R.; Mathieu, M.; Simon, B. *C. R. Acad. Sci. Paris* **1972**, *274*, 473−476. (b) Boistelle, R.; Mathieu, M.; Simon, B. *Surf. Sci.* **1974**, *42*, 373−388.
(38) de Leeuw, N. H.; Parker, S. *J. Chem. Soc., Faraday Trans.* **1997**, *93*, 467−475.
(39) Titiloye, J. O.; Parker, S. C.; Mann, S. *J. Cryst. Growth* **1993**, *131*, 533−545.
(40) Zemann, J. *Acta Crystallogr.* **1957**, *10*, 664−666.
(41) Pastero, L.; Aquilano, D.; Genovese, A.; Costa, E., to be submitted to *J. Cryst. Growth*.
(42) Hartman, P.; Kern R. *C. R. Acad. Sci. Paris*, **1964**, *258*, 4591−4593.
(43) Nielsen, A. E.; Toft, J. M. *J. Cryst. Growth* **1984**, *67*, 278−288.
(44) van der Voort, E.; Hartman, P. *J. Cryst. Growth* **1990**, *104*, 450−456.
(45) Christoffersen, J.; Christoffersen, M. *J. Cryst. Growth* **1990**, *100*, 203-211.
(46) Teng, H. H.; Dove, P. M.; Orme, C. A.; De Yoreo, J. J. *Science* **1998**, *282*, 724−727.
(47) Lundager Madsen, H. E. *J. Cryst. Growth* **1995**, *152*, 94−100.

CG034217R